

# IBM Research Report

## A Study of the Effects of Solder Volume on the Interfacial Reactions in Solder Joints Using Differential Scanning Calorimetry Technique

**Won Kyoung Choi, Sung K. Kang, Da-Yuan Shih**

IBM Research Division

Thomas J. Watson Research Center

P.O. Box 218

Yorktown Heights, NY 10598



Research Division

Almaden - Austin - Beijing - Delhi - Haifa - India - T. J. Watson - Tokyo - Zurich

## **Abstract**

Differential scanning calorimetry (DSC) technique was employed to understand the interfacial reactions during soldering by simulating the soldering process as well as analyzing the interfacial reactions. The measurement of peak temperatures and heat involved provides useful information about the interfacial reactions such as the amount of intermetallic compounds (IMC) formed and that of Cu dissolved. Sn-plated Cu balls with a different Sn thickness were used to investigate the solder volume effect. As the Sn layer thickness decreases, the amount of IMC formed during reflow increases in general. This suggests IMC formation depends on the Sn volume. In addition, a Ni layer (electroless and electroplated) introduced as a diffusion barrier between Cu and Sn was found effective in reducing Cu out diffusion. The results from the DSC study were confirmed by the conventional metallography and SEM/EDX techniques.

Key Words ; differential scanning calorimetry (DSC), tin coating, electroplated Ni, electroless Ni-P, solder volume, interfacial reactions, intermetallic compounds, dissolution

## Introduction

The solder joints play important roles in the electronic packages, serving both as electrical interconnections between components and a mechanical support of components. As electronic packages are continuing to get smaller in size and more integrated, fine-pitch solder joints are required and therefore the reliabilities of the solder joints become more critical. One important factor influencing the solder joint reliability is the interfacial reaction between the molten solder and the substrate during soldering. For example, A copper pad on printed circuit board dissolves into molten solder and forms intermetallic compounds (IMC) during reflow joining. This would make a significant impact on solder joint properties, such as solder composition, microstructure, and mechanical properties.

The formation and growth kinetics of the IMC in various solder joints have been investigated extensively [1-6]. Generally, in solid-state reactions, such as annealing at an elevated temperature, the IMC grows in a rather planar morphology and its growth rate follows Fick's 1st law of diffusion [3,5,7]. In this situation, the driving force for IMC growth is only the concentration gradient of the diffusing element in the IMC layer and in the solder. On the other hand, the interfacial reactions during the soldering depend on several factors, such as solubility of a solute metal in a liquid solder, dissolution rate of a surface finish into a liquid solder, solder volume, surface finish layer thickness, and others [7-9]. The interpretation of the interfacial reactions during soldering is therefore more complicated. For example, the IMC growth kinetics cannot be described by a simple relationship between the IMC thickness and time.

It has been reported that there is an intermediate time period in the IMC growth between a molten solder and a substrate [7-9]. Kang and Ramachandran [8] found a reduced growth of the nickel-tin intermetallic layers at intermediate reaction times in the liquid tin-solid nickel system. Schaeffer et al. [9] have suggested the growth of interfacial intermetallic layers in the liquid Sn-Pb and solid copper system decreases at intermediate reaction times because the dissolution rate of IMC is balanced with its growth rate. In addition, Choi and Lee [7] also confirmed the presence of the intermediate period in the IMC growth by analyzing copper composition in the reacted solder. These studies indicate that the IMC growth is closely related to the dissolution phenomena, which would change the composition and microstructure of solder joints.

Under the condition of the same reflow temperature and time, the dissolution may be affected by a solder joint size, such as solder volume, thickness of surface finish layers and pad size [9-10]. A solder joint size must be different depending on its applications, such as, ball grid array (BGA), chip-scale package (CSP), and flip chip. The different solder joint size changes the amount of diffusing atoms and so IMC growth kinetics. The dependence of the dissolution on the solder volume has been reported previously [9-11]. However, it was not easy to explain clearly the relationship between the solder volume and IMC growth kinetics.

To control the dissolution of a surface finish layer, a diffusion barrier layer such as Ni is introduced. Depending on the kind of plating methods, electroless or electrolytic, the Ni layer yields the different interfacial reactions [12]. Therefore, the comparison study of the interfacial reactions between the electroless and electroplated Ni layers is also performed.

The interfacial reactions have been studied by employing various experimental techniques to directly measure IMC thickness, solder composition, dissolution of a base metal and others. Kang et al. [13] successfully employed Differential Scanning Calorimetry (DSC) technique to investigate the interfacial reaction kinetics during soldering as well as in solid-state aging. By extending the DSC method, it can also measure the interfacial reactions in the samples that are too difficult to be investigated by other methods. For example, the amount of dissolved solutes into a solder is often too small to be detected by EDX or WDX. However, the compositional change of a molten solder can be measured by DSC with the liquidus temperature of the solder. In addition, the thickness of the IMCs formed in a solder joint could be estimated from the heat generated during the melting of the IMC [13].

## **Experimental procedure**

In this study, DSC technique was utilized to simulate a soldering process and to analyze the interfacial reactions. The peak temperatures and heat involved were measured to obtain the information about the amount of IMC formed and that of Cu dissolved. Sn-plated Cu balls with a different Sn thickness were used to investigate the solder volume effect. In addition, a Ni barrier layer (electroless or electrolytic) was introduced between Cu and Sn to investigate its role in suppression of the dissolution of Cu into molten Sn. Metallography was combined with SEM/EDX to verify the DSC results.

Cu balls (889  $\mu\text{m}$  diameter) were plated with Sn and/or Ni using an equipment described

elsewhere [14]. Sn plating was performed in a Lea Ronal Sn plating solution with a current density of approximately  $87 \text{ mA/cm}^2$  for various times depending on a target Sn thickness. The Sn solder volume was estimated from the plated Sn layer thickness and the surface area of a Cu ball ( $2.48 \times 10^6 \text{ } \mu\text{m}^2$ ). For three Sn thicknesses chosen (40, 10, and 5  $\mu\text{m}$ ), the volume ratio is calculated as 8.6:2.0:1.0 and the volume to area ratios are 0.175, 0.0403, and 0.0204 cm, respectively. A Ni barrier layer was deposited between the Cu ball and Sn layer by either electrolytic or electroless process. Electrolytic Ni plating was performed in a nickel sulfamate solution with  $5.3 \text{ A/dm}^2$ . All electroless Ni layers have approximately 8wt% P content. The Ni thickness was chosen to be 1 and 2  $\mu\text{m}$ .

The DSC unit used is a thermal analysis system, DSC220, from Seiko Instruments, Inc. A sealed aluminum pan is used to hold Sn-coated Cu balls of 40 to 45 mg. Figure 1 represents a typical heating schedule used in the DSC study. Fig. 1a is to examine the effects of the solder volume on interfacial reactions by measuring the amount of IMC formed. A sample kept at  $250 \text{ }^\circ\text{C}$  for a different times from 10 to 40 min followed by heating up to  $450 \text{ }^\circ\text{C}$  to pass the melting temperature of the IMC,  $\eta\text{-Cu}_6\text{Sn}_5$ ,  $415 \text{ }^\circ\text{C}$ . The heat generated during melting of the IMC is measured to calculate IMC thickness [13]. In order to evaluate the effects of a Ni barrier layer on the interfacial reactions, the melting point of Sn was measured during the second heating after the reflow for 10 to 60 min as shown in Fig 1b. To reduce the additional interface reactions, a fast cooling was provided after the reflow. A change in the melting point of Sn layer is related to the amount of Ni and Cu dissolved into the molten Sn solder.

During all DSC experiments, choosing optimum heating and cooling rates is important.

For example, slow heating may cause undesirable dissolution and fast heating can yield incomplete melting of IMC. From several preliminary experiments, an optimum heating rate was such as 20 °C/min for the peak temperature measurement of Sn in Fig. 1b, and 10 °C/min to detect the heat generated, in Fig 1a.

## Results

Figure 2 shows a typical DSC scan from room temperature to 450°C with Sn-coated Cu balls having 40 μm Sn. A small exothermic peak at 250 °C is due to the time delay in plotting for a reflow time. During heating, two endothermic peaks were observed; one at about 229 °C and another at around 409 °C. The peak at 229 °C is associated with the melting of Sn layer and the peak at 409 °C from melting of the η-Cu<sub>6</sub>Sn<sub>5</sub> phase, which was formed during the reflow at 250 °C. Thus the total amount of the η-Cu<sub>6</sub>Sn<sub>5</sub> formed during reflow can be estimated from this peak. The peak size of the η-Cu<sub>6</sub>Sn<sub>5</sub> phase is very small compared to the Sn peak because its relative volume is much less than the Sn layer. The method to calculate the thickness of the η-Cu<sub>6</sub>Sn<sub>5</sub> phase has been reported by Kang et al. [13]. The following equations including an enthalpy of fusion of the η-Cu<sub>6</sub>Sn<sub>5</sub> phase are used;

$$\eta\text{-Cu}_6\text{Sn}_5(\text{wt}) = \text{Vol}(\eta\text{-Cu}_6\text{Sn}_5) \times \rho(\eta\text{-Cu}_6\text{Sn}_5) \times \text{total number of Cu balls} \quad (1)$$

$$\eta\text{-Cu}_6\text{Sn}_5(\text{wt}) = (\rho(\eta\text{-Cu}_6\text{Sn}_5) / \rho(\text{Cu})) (\text{Vol}(\eta\text{-Cu}_6\text{Sn}_5) / \text{Vol}(\text{Cu ball})) \quad (2)$$

The weight fraction of η-Cu<sub>6</sub>Sn<sub>5</sub> phase formed at the interface between a Cu ball and a

Sn layer is calculated by dividing the measured heat of fusion during melting of the  $\eta$ -Cu<sub>6</sub>Sn<sub>5</sub> phase by the enthalpy of fusion of  $\eta$ -Cu<sub>6</sub>Sn<sub>5</sub> phase, 86.4 J/g [13]. The density of the  $\eta$ -Cu<sub>6</sub>Sn<sub>5</sub>,  $\rho(\eta\text{-Cu}_6\text{Sn}_5)$ , is 8.28 g/cm<sup>3</sup> [15,16] and the density of Cu,  $\rho(\text{Cu})$ , 8.96 g/cm<sup>3</sup> [15, 17]. The diameter of Cu ball is 889  $\mu\text{m}$ . By solving eq. 1 and 2, the amount of IMC formed could be estimated.

Table I lists the calculated thickness of the  $\eta$ -Cu<sub>6</sub>Sn<sub>5</sub> as a function of the reflow time for the 40  $\mu\text{m}$  Sn layer (Cu/Sn(40)). As the reflow time becomes longer, the amount of heat measured during the  $\eta$ -Cu<sub>6</sub>Sn<sub>5</sub> melting increases, indicating an increase in the calculated thickness. The calculated thickness is compared with the  $\eta$ -Cu<sub>6</sub>Sn<sub>5</sub> thickness measured from the cross-sectioned samples reflowed for 10 and 20 min in Fig. 3. These samples were prepared just after the first heating schedule without an additional heating. The IMC morphology looks like an irregular scallop type. The thickness range of IMCs was measured from each cross-section and compared to those measured from DSC, in Table I. A reasonable agreement between the calculated and measured thicknesses was obtained, demonstrating that the DSC technique is very useful to study the interfacial reaction in a simulated condition. Above all, it can measure the total amount of IMCs formed in a solder joint including the IMCs dispersed in the solder matrix as well as the interfacial IMC.

The IMC thicknesses for the samples having 10  $\mu\text{m}$  Sn layer (Cu/Sn(10)) are listed in Table II. After 20 min reflow, the second IMC,  $\epsilon$ -Cu<sub>3</sub>Sn phase, was observed. The apparent IMC thickness measured from cross-section therefore includes the total thickness of both  $\eta$ -Cu<sub>6</sub>Sn<sub>5</sub> and  $\epsilon$ -Cu<sub>3</sub>Sn. Thus the thickness of  $\eta$ -Cu<sub>6</sub>Sn<sub>5</sub> phase was only



compared with the calculated IMC thickness by DSC, while the total IMC thickness was also listed in Table II and III. The calculated thickness from DSC is a somewhat higher than the measured because it may include the  $\eta$ -Cu<sub>6</sub>Sn<sub>5</sub> phase formed in the solder matrix. However, the general trends of both the calculated and measured thickness with the reflow time are similar to each other.

The thickness of the  $\eta$ -Cu<sub>6</sub>Sn<sub>5</sub> phase calculated for the 5  $\mu$ m Sn layer (Cu/Sn(5)) is listed in Table III. The IMC thickness for the 5  $\mu$ m Sn layer was much less than those for 10  $\mu$ m Sn and 40  $\mu$ m Sn listed in Table I and II. Figure 4 presents a SEM micrograph (secondary electron image) of the cross-section from the 5  $\mu$ m sample for 40 min reflow. The IMC morphology looks less irregular, more planar or a layer shape, with an apparent thickness of 3.5 ~ 4  $\mu$ m. An energy Dispersive X-ray (EDX) analysis has been performed to confirm the identity of the IMC phases formed at the interface. Figure 5 exhibits the EDX spectra for the 5  $\mu$ m Sn (Fig. 5a) and 40  $\mu$ m Sn (Fig. 5b). For the 5  $\mu$ m Sn sample, the  $\epsilon$ -Cu<sub>3</sub>Sn phase is a majority over the  $\eta$ -Cu<sub>6</sub>Sn<sub>5</sub>. This explains why the calculated IMC ( $\eta$ -Cu<sub>6</sub>Sn<sub>5</sub>) is so small for the 5  $\mu$ m Sn compared to others.

Figure 6 shows the peak temperature variation with reflow time for 40  $\mu$ m Sn sample. As a reference, the melting temperature of pure Sn was measured at 233.5 °C, which is a little higher than 232 °C, the reported value [18]. In Cu/Sn(40), the peak temperature is lowered to 227 °C in 20 min. This temperature is similar to the eutectic temperature of Sn-0.7Cu. At the “0” time, the temperature observed is lower than the pure Sn peak, implying some Cu atoms diffused already into the solid Sn layer during the heating period.

Figure 7 shows the peak temperature variations with the reflow time for Sn-Ni-coated Cu balls. The Ni layer is either electro- or electroless deposited. All samples tested have a 40  $\mu\text{m}$  Sn layer on a Cu ball. In the label, “EN4” represent a 4  $\mu\text{m}$  electroless Ni-P and “ED2” a 2  $\mu\text{m}$  electroplated Ni layer. As the reflow time increases from 10 to 60 min, the peak temperature goes down in all samples except for “ED1”. When an electroless Ni-P layer is introduced between the Sn layer and Cu ball, the peak temperature is generally reduced as the reflow time increases. However, for the 4  $\mu\text{m}$  Ni layer (EN4), the temperature does not change in 20 min and only decreases slightly after 20 min. In the samples with 2  $\mu\text{m}$  Ni (EN2), the temperature is reduced in 20 min and not much changed thereafter. In the samples with 1  $\mu\text{m}$  Ni (both EN1 and ED1), it decreases abruptly in 10 min and then slowly approaches to 228 °C.

## Discussions

### *Effects of the Solder Volume on Interfacial Reactions*

The interfacial reaction during reflow takes place through the mass transport phenomena. The Cu diffuses into molten solder by means of the chemical potential gradient between solder and substrate. Hence, the volume of solder and thickness of a surface finish layer, have a significant bearing on the interfacial reaction. To demonstrate the solder volume effects on interfacial reactions, the IMC thickness estimated from the DSC study was plotted in Fig. 8 for Cu/Sn(40) and Cu/Sn(10). Only after 10 min, the IMC in Cu/Sn(10)

grows three times thicker than that in Cu/Sn(40). This difference in the IMC growth rate can be explained by the dissolution of Cu into the molten Sn during the reflow. It takes much shorter time for the Sn solder to be saturated with the dissolved Cu in Cu/Sn(10) than in Cu/Sn(40). The saturated solder with Cu can provide a higher flux of Cu atoms to be incorporated in the IMC growth at the interface. In addition, the saturated solder would not dissolve away the IMC at the interface, while the undersaturated solder would dissolve the IMC itself. Thus the IMC in Cu/Sn(10) could grow more than that in Cu/Sn(40).

The effects of solder volume or joint size on the interfacial reactions have been one of the interesting topics so far [9, 10, 20, 21]. Among those, Schaefer et al [9] reported that the ratio ( $V/A$ ) of solder volume to contacted area controlled on the dissolution phenomena. They explained that it was caused by a longer diffusion distance for Cu to saturate the molten solder with an increase in the value of  $V/A$ . This explanation could be applied for the present study. The volume of 40  $\mu\text{m}$  Sn layer is 4.35 times larger than 10  $\mu\text{m}$  Sn. Since the interfacial area between the molten solder and Cu ball in both cases is same,  $(V/A)_{40\mu\text{m}}$  is 4.35 times larger than  $(V/A)_{10\mu\text{m}}$ . It means that the distance for Cu diffusion in Cu/Sn(40) is 4.35 times longer than in Cu/Sn(10), and so the corresponding interfacial reactions would behave differently.

The formation of the second IMC phase,  $\epsilon\text{-Cu}_3\text{Sn}$ , may alter the  $\eta\text{-Cu}_6\text{Sn}_5$  growth kinetics, as confirmed in Fig. 5. The  $\text{Cu}_3\text{Sn}$  grows by consuming the  $\eta\text{-Cu}_6\text{Sn}_5$  phase layer in Cu/Sn(10) after 20 min, which it was observed in Cu/Sn(40) only after 40 min. This indicates that the formation and growth of the  $\epsilon\text{-Cu}_3\text{Sn}$  phase are also dependent on

the solder volume. The calculated IMC thickness in Cu/Sn(5) is very small in Table III, even though the Sn layer can be saturated much quickly. In this case, the formation of  $\epsilon$ -Cu<sub>3</sub>Sn may be triggered earlier than other cases because the saturated solder may provide a very high flux of Cu atoms. Thus the remaining  $\eta$ -Cu<sub>6</sub>Sn<sub>5</sub> phase is much smaller in quantity and further reduced gradually as the reflow time increases. Since the  $\epsilon$ -Cu<sub>3</sub>Sn grows by consuming the  $\eta$ -Cu<sub>6</sub>Sn<sub>5</sub> layer formed first [22], the decrease in the  $\eta$ -Cu<sub>6</sub>Sn<sub>5</sub> thickness in Cu/Sn(10) after 20 min in Figure 8 may attributed to the formation of  $\epsilon$ -Cu<sub>3</sub>Sn.

In Fig. 6, the Sn peak temperature of the 40  $\mu$ m Sn decreases to its minimum,  $\sim 227$  °C, close to the Sn-0.7Cu eutectic temperature. After 20 min, the Sn peak temperature is steadily increases. This is explained by the higher Cu solubility at 250 °C than at 227 °C, which requires more Cu atoms to dissolve into the molten Sn at 250 °C.

### **Effect of Ni Barrier Layers on Cu Diffusion**

As soon as a solder melts on the substrate during reflow, the substrate tends to dissolve into the molten solder and the IMC forms at the same time. In general, the reaction rate of the IMC formation is too fast to be a rate controlling-step in the IMC growth equation [23]. When a Ni layer is used as a diffusion barrier on the substrate Cu, it is the Ni layer to react first with the molten solder. Depending on the type of a Ni layer, such as, electroless or electroplated, the interfacial reactions would be different. Kang et al [12] reported that the dissolution of an electroless Ni-P layer was faster than that of an electrolytic Ni layer, and their IMC growth kinetics were also different. In another study,

the effect of an electroplated Ni thickness on interfacial reactions was reported [21], where the cross-sectioned joints were analyzed by EPMA technique to detect a small difference in composition of the solder, but without much success. In this study, by detecting the change in its melting point of a molten solder by DSC, it was possible to investigate the diffusion of a solute into a molten solder or through a Ni diffusion barrier layer. This study has also provided the information on the Ni thickness, which can effectively reduce the Cu out diffusion. For 1  $\mu\text{m}$  Ni thickness, Cu diffusion as well as Ni dissolution into a molten solder happens in a short time. Thus the peak temperature goes down near to the Sn-Cu eutectic temperature, 227  $^{\circ}\text{C}$ . It is also confirmed by EDX analysis that the IMC formed at the interface has a Sn-Cu-Ni ternary composition, indicating Cu atoms diffused through the Ni layer and dissolved into the molten solder. When a Ni layer is thicker than 2  $\mu\text{m}$ , Ni dissolves first into a molten solder and the Sn-Ni IMC forms before Cu diffuses through the Ni layer. Thus the peak temperature does not change much compared to 1  $\mu\text{m}$  Ni layer. And the IMC remains as  $\text{Ni}_3\text{Sn}_4$ . However, as the reflow time increases to 60 min, Cu diffuses through the Ni layer and transforms the Ni-Sn IMC into a ternary Sn-Ni-Cu IMC as shown in Figure 9. The Ni-Sn IMC changes into the Cu-Sn-Ni ternary phase after 60 min in Cu/Ni(EL2)/Sn, while the IMC in Cu/Ni(EL1)/Sn is already the Cu-Sn-Ni ternary phase after 20 min. It suggests that the Cu could diffuse through 1  $\mu\text{m}$  Ni layer in 20 min, while it could not diffuse through 2  $\mu\text{m}$  Ni (electroless) in 20 min. Thus it is recommended that a Ni layer thickness should be at least 2  $\mu\text{m}$  in order to reduce Cu atoms diffusing into the molten solder for 20 min at 250  $^{\circ}\text{C}$ .

### *Difference between Electroless and Electroplated Ni Barrier Layers*

In Fig. 7, for 1  $\mu\text{m}$  Ni layer, the melting temperature of Sn in both electroplated and electroless Ni layer is reduced at a similar rate. However, in 2  $\mu\text{m}$  Ni, the melting point of Sn is reduced more quickly in the electroless Ni-P layer. Especially, the change of Sn peak in 2  $\mu\text{m}$  electroplated Ni is less than 4  $\mu\text{m}$  electroless Ni-P in 20 min. This means that the Ni dissolution is easier from the electroless Ni-P layer than from the electroplated Ni. In fact, this result is consistent with the observation that the dissolution rate of Ni is faster with electroless Ni-P than electroplated Ni [12]. It may be due to the difference in the microstructure of Ni layer. It has been found an electroless Ni-P layer composed of fine grains [24] and an electroplated Ni having columnar structures or larger grains [19]. The microstructure composed of finer grains has a larger grain boundary area, thus more defects in the layer. The dissolution of Ni from an electroless Ni-P layer can therefore happen easily during the reflow. This may explain why the change of the Sn peak happens more quickly in the electroless Ni-P in 20 min than the electroplated Ni. Accordingly, an electroplated Ni layer is regarded to be more effective than an electroless Ni-P in terms of a diffusion barrier during soldering.

## **Conclusions**

1. The differential scanning calorimetry (DSC) technique has been successfully employed to understand the interfacial reactions during soldering. This method enables to measure the amount of IMC formed, the amount of solute atoms dissolved into a solder and the

effectiveness of a diffusion barrier layer.

2. By measuring the amount of IMC formed during reflow using DSC technique, it is demonstrated that the interfacial reactions depend on the solder volume of a joint, influenced by the dissolution phenomena. The IMC growth rate is much larger in 10  $\mu\text{m}$  Sn on a Cu ball than in 40  $\mu\text{m}$  Sn. However, the amount of  $\eta\text{-Cu}_6\text{Sn}_5$  in 5  $\mu\text{m}$  Sn is much smaller than in other samples. This is due to the formation of the second IMC,  $\epsilon\text{-Cu}_3\text{Sn}$  in the smaller volume of the Sn layer.

3. The effectiveness of a Ni layer as a diffusion barrier between solid Cu and molten Sn is evaluated by measuring the change in the melting temperature of Sn. The melting temperature reduction is observed as a reflow time increases due to the dissolution of Ni or Cu. It is found that a Ni layer thickness should be at least 2  $\mu\text{m}$  to effectively reduce the off diffusion of Cu. An electroplated Ni is found to be more effective than an electrolytic Ni.

#### Acknowledgements

The authors are grateful to C. Sambucetti and Y.-T. Cheng (IBM Research) for help with electroless Ni-P plating and N. Labianca (IBM Research) for help with differential scanning calorimetry.

## References

1. M. Onishi and H. Fujibuchi, *Trans. JIM* 16, 539 (1975).
2. Y. Wu, J. A. Sees, C. Pouraghabagher, L. A. Foster, J. L. Marshall, E. G. Jacobs and R. F. Pinizzotto, *J. Electron. Mater.* 22, 769 (1993).
3. K. L. Erickson, P. L. Hopkins and P. T. Vianco, *J. Electron. Mater.* 23, 729 (1994).
4. Z. Mei, A. J. Sunwoo and J. W. Morris, Jr., *Met. Trans.* 23A, 857 (1992).
5. P. T. Vianco, P. F. Hlava and A. C. Kilgo, *J. Electron. Mater.* 23, 583 (1994).
6. P. T. Vianco, K. L. Erickson and P. L. Hopkins, *J. Electron. Mater.* 23, 721 (1994).
7. W. K. Choi and H. M. Lee, *J. Electron. Mater.* 29, 1207 (2000)
8. S. K. Kang and Ramachandran, *Scripta Metall.* 14, 421 (1980).
9. M. Schaefer, W. Laub, R. A. Fournelle and J. Liang, *Proceedings of the Design and Reliability of Solders and Solder Interconnects* ed. By R. K. Mahidhara, D. R. Frear, S. M. L. Sastry, K. L. Murty, P. K. Liaw and W. L. Winterbottom, TMS, Warrendale, pp. 247 (1997).
10. B. Salam, N. N. Ekere and D. Rajkumar, *Proc. 51<sup>st</sup> Elec. Comp. Tech. Conf.*, *Proc. 51<sup>st</sup> Elec. Comp. Tech. Conf. Orlando, FL.*, pp. 471 (2001).
11. I. Okamoto and T. Yasuda, *Transactions of JWRI.* 15, 245 (1986).



12. S. K. Kang, D.Y. Shih, K. Fogel, P. Lauro, M. J. Yim, G. Advocate, M. Griffin, C. Goldsmith, D. W. Henderson, T. Gosselin, D. King, J. Konrad, A. Sarkhel and K. J. Puttlitz, Proc. 51<sup>st</sup> Elec. Comp. Tech. Conf. Orlando, FL., pp. 448 (2001).
13. S. K. Kang and S. Purushothaman, J. Electron. Mater. 27, 1199 (1998)
14. S. K. Kang, S. Purushothaman, and R. S. Rai, US patent number 6059952 (1998).
15. P. E. Davis, M. E. Warwick and P. J. Kay, "Plating and Surface Finishing", pp. 72 (1982)
16. R. J. Fields, S. R. Low III and G. K. Lucey, Jr., The Metal Science of Joining, ed. M. J. Cieslak, et al., Warrendale, PA, TMS, pp.165 (1991),.
17. CRS Handbook of Chemistry and Physics, ed. D. R. Lide, 73<sup>rd</sup> Ed., Boca Raton, FL., CRC Press, (1992-1993).
18. T. B. Massalski, Binary Alloy Phase Diagrams, 2nd ed., ASM, Materials Park (1992).
19. William H. Safranek, "The Properties of Electrodeposited Metals and Alloys" A Handbook, Elsevier, pp. 278 (1974)
20. I. Kawakatsu and H. Yamaguchi, J. Jap. Ins. Met. 31, 1387 (1967).
21. W. K. Choi and H. M. Lee, J. Electron. Mater. 28, 1251 (1998).
22. U. Gosele and K. N. Tu, J. Appl. Phys. 53, 3252 (1982).
23. B.-J. Lee, N.-M. Hwang and H. M. Lee, Acta. Mater. 45, 1867 (1997).

24. P. L. Liu, Z. Xu and J. K Shang, *Metall. Mater. Trans.* 31A, 2857 (2000).

**Table I. Calculated and Measured Thickness of  $\eta$ -Cu<sub>6</sub>Sn<sub>5</sub>  
as a Function of Reflow Time for 40  $\mu$ m Sn**

<b>Reflow Time (min)</b>	<b>Peak Temperature (°C)</b>	<b>Heat (mJ/g)</b>	<b>IMC Thickness from DSC (<math>\mu</math>m)</b>	<b>IMC Thickness by Cross-section (<math>\mu</math>m)</b>
10	409.1	1697.5	3.1	1.6-9
20	408.9	1720.8	3.2	3-8
30	408.8	1865.4	3.5	-
40	408.4	2315.6	4.3	-

**Table II. Calculated and Measured Thickness of  $\eta$ -Cu<sub>6</sub>Sn<sub>5</sub>  
as a Function of Reflow Time for 10  $\mu$ m Sn**

<b>Reflow Time (min)</b>	<b>Peak Temperature (°C)</b>	<b>Heat (mJ/g)</b>	<b>IMC Thickness from DSC (<math>\mu</math>m)</b>	<b>IMC Thickness by Cross-section (<math>\mu</math>m)</b>
10	408.4	5206.0	9.6	1.6-8.2
20	408.3	7243.8	13.4	2.2-10.6
30	408.4	6848.6	12.6	2.3-10.4 (total 4-12)
40	408.8	6223.7	11.5	2-10 (total 4-12)

**Table III. Calculated and Measured Thickness of  $\eta$ -Cu<sub>6</sub>Sn<sub>5</sub>  
as a Function of Reflow Time for 5  $\mu$ m Sn**

<b>Reflow Time (min)</b>	<b>Peak Temperature (°C)</b>	<b>Heat (mJ/g)</b>	<b>IMC Thickness from DSC (<math>\mu</math>m)</b>	<b>IMC Thickness by Cross-section (<math>\mu</math>m)</b>
10	405.9	303.7	0.56	2.4 ( total 3.4)
20	405.6	487.1	0.90	1.8 (total 3.8)
30	405.8	464.8	0.86	1.0 (total 4.2)
40	405.8	500.5	0.93	1.2 (total 4.4)

## Figure Captions

**Figure 1 Thermal profiles employed in DSC experiments ; (a) for solder volume effects and (b) of Ni diffusion barrier layers.**

**Figure 2 A typical DSC scan from room temperature to 450°C with a sample of 40  $\mu\text{m}$  Sn.**

**Figure 3 Optical micrographs of the cross-sectioned samples having 40  $\mu\text{m}$  Sn layer with the reflow time ; (a) 10 min, and (b) 20 min**

**Figure 4 SEM micrograph of a cross-sectioned sample having 5  $\mu\text{m}$  Sn layer for 40 min reflow.**

**Figure 5 Energy Dispersive X-ray spectra from the cross-sectioned samples ; (a) 5  $\mu\text{m}$ , and (b) 40  $\mu\text{m}$  Sn.**

**Figure 6 The variation of melting temperatures in Cu/Sn(40) balls as a function of reflow time.**

**Figure 7 The variation of melting temperatures in Cu/Sn balls with an electrolytic Ni and electroless Ni-P layers as a function of reflow time and Ni layer thickness.**

**Figure 8 The thickness of the  $\eta\text{-Cu}_6\text{Sn}_5$  phase formed at 250 °C as a function of reflow time in Cu/Sn(10) and Cu/Sn(40).**

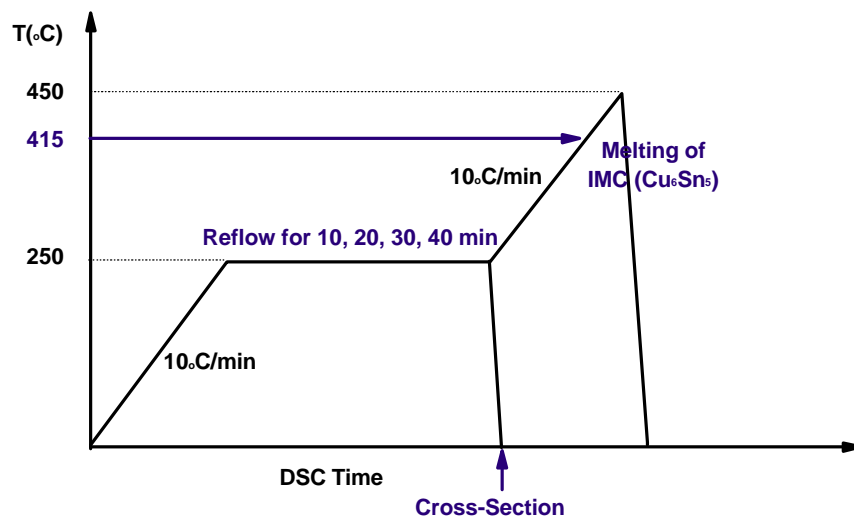
**Figure 9 EDS spectra of IMCs in Cu/Ni(ED1)/Sn after (a) 20 min and (b) 60 min, and IMCs in Cu/Ni(ED2)/Sn after (c) 20 min, and (d) 60 min.**

## Tables

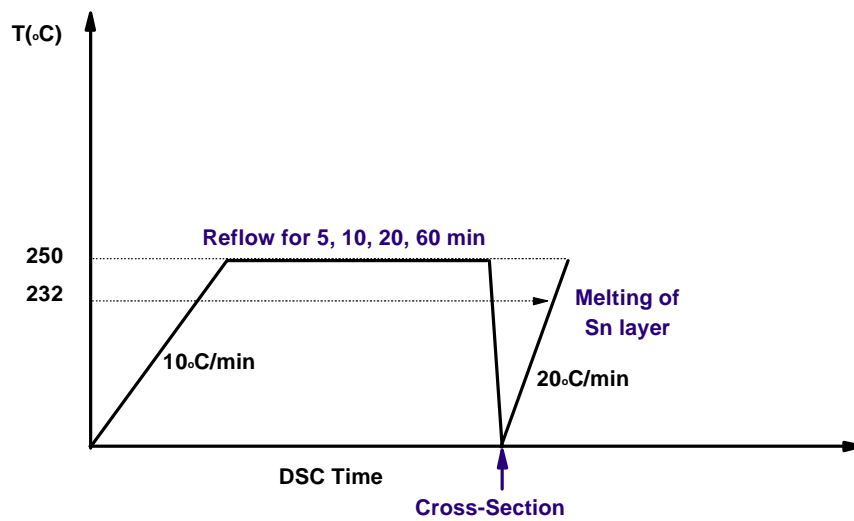
**Table I. Calculated and Measured Thickness of  $\eta$ -Cu<sub>6</sub>Sn<sub>5</sub> as a Function of Reflow Time for 40  $\mu$ m Sn**

**Table II. Calculated and Measured Thickness of  $\eta$ -Cu<sub>6</sub>Sn<sub>5</sub> as a Function of Reflow Time for 10  $\mu$ m Sn**

**Table III. Calculated and Measured Thickness of  $\eta$ -Cu<sub>6</sub>Sn<sub>5</sub> as a Function of Reflow Time for 5  $\mu$ m Sn**



a



b

Figure 1 Thermal profiles employed in DSC experiments ; (a) for solder volume effects and (b) for of Ni diffusion barrier layers.



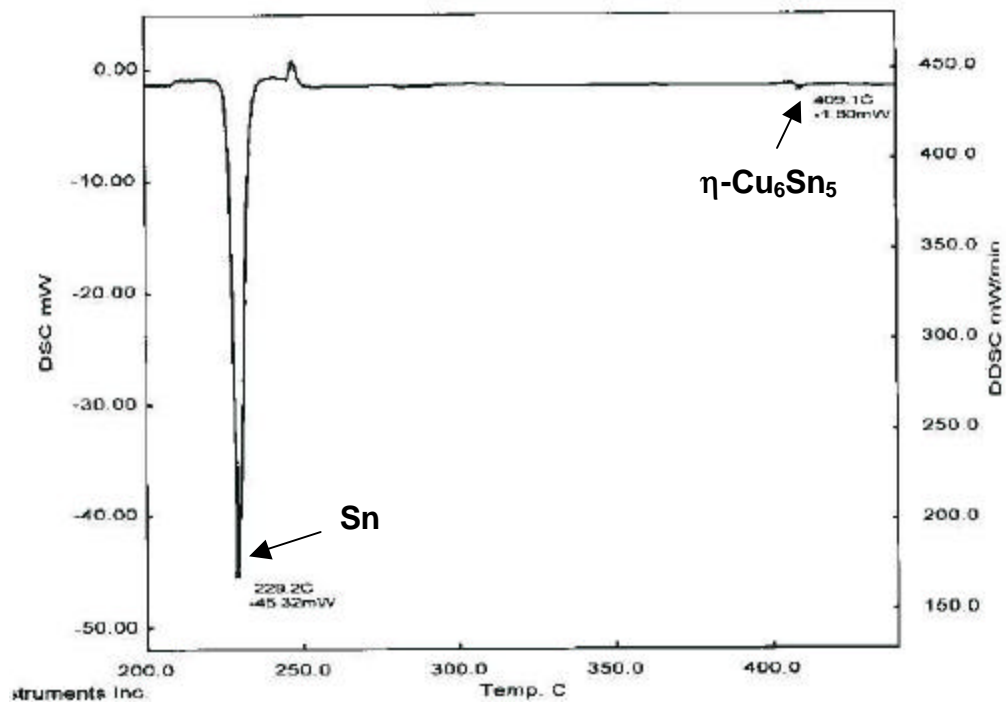
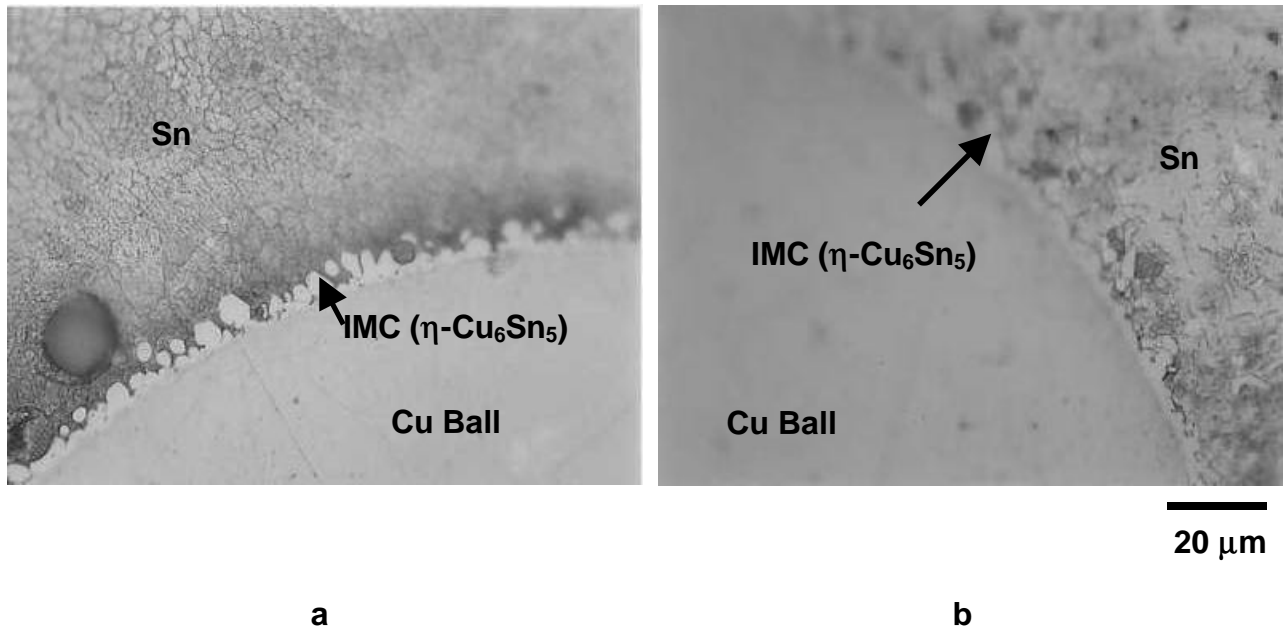
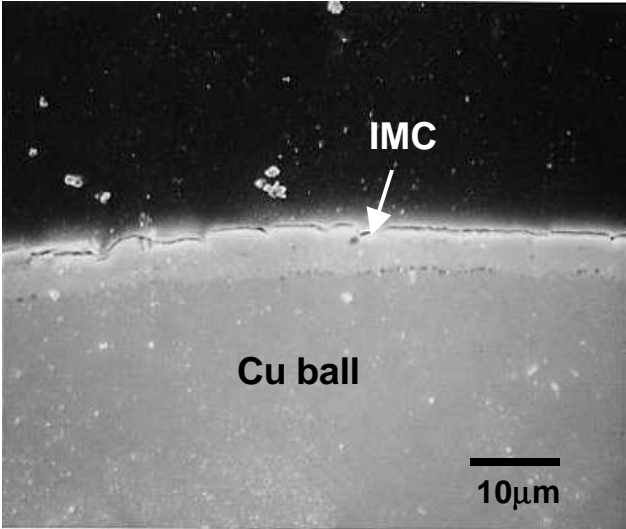


Figure 2 A typical DSC scan from room temperature to 450°C with a sample of 40 μm Sn.



**Figure 3 Optical micrographs of the cross-sectioned samples having 40 μm Sn layer with the reflow time ; (a) 10 min, and (b) 20 min**



**Figure 4 SEM micrograph of a cross-sectioned sample having 5 µm Sn layer for 40 min reflow.**

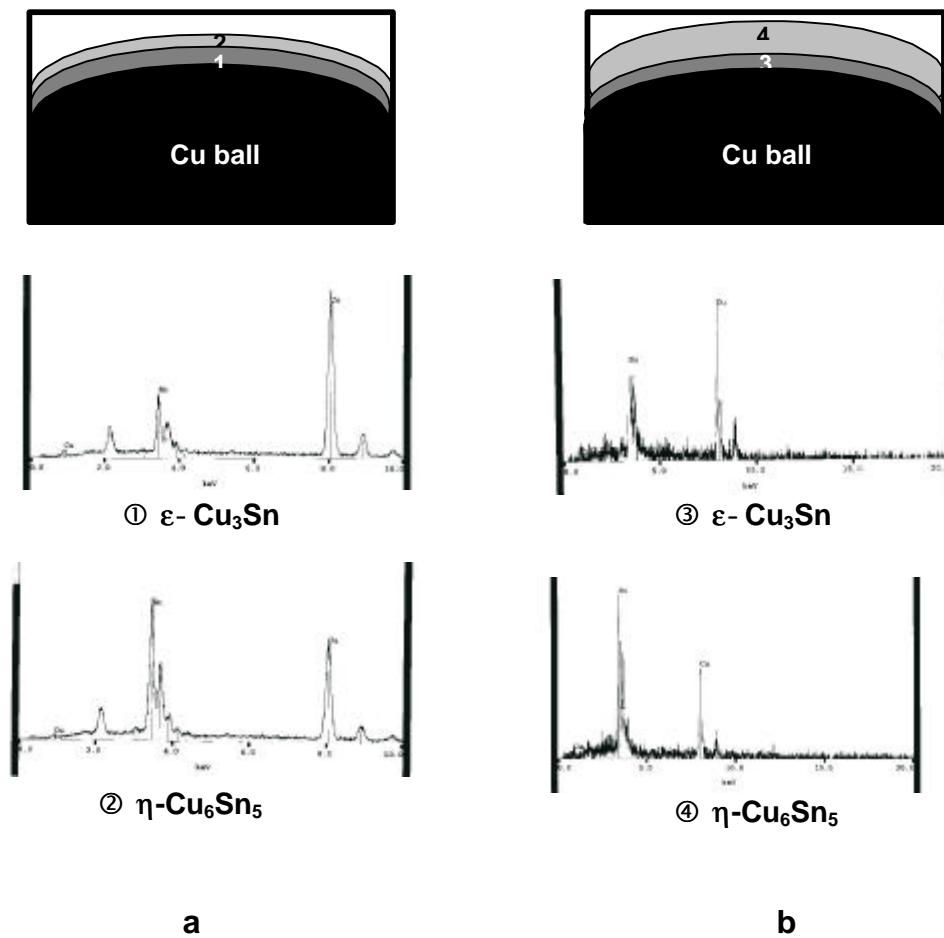
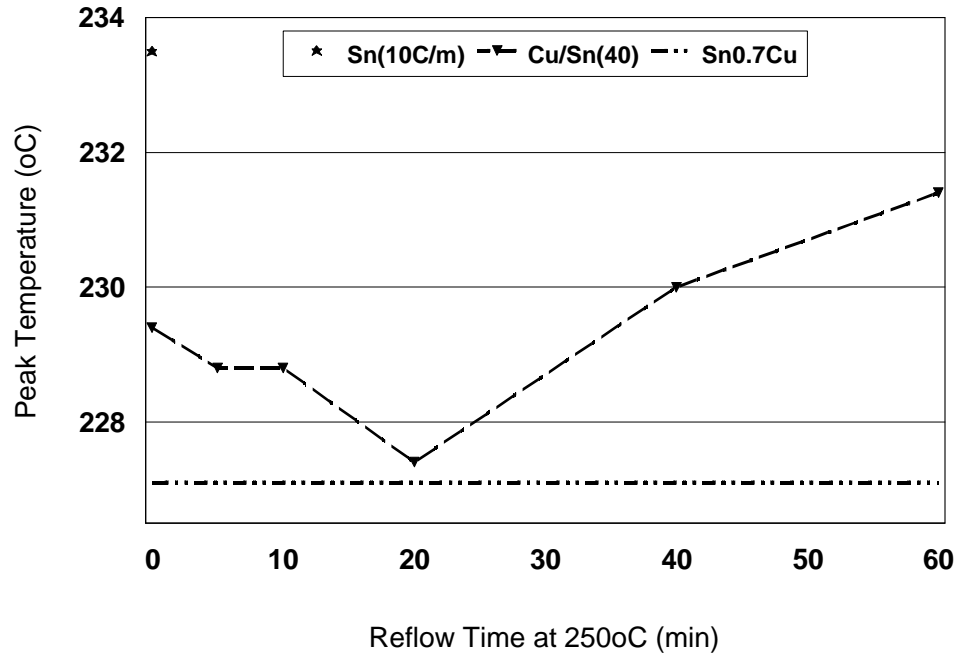
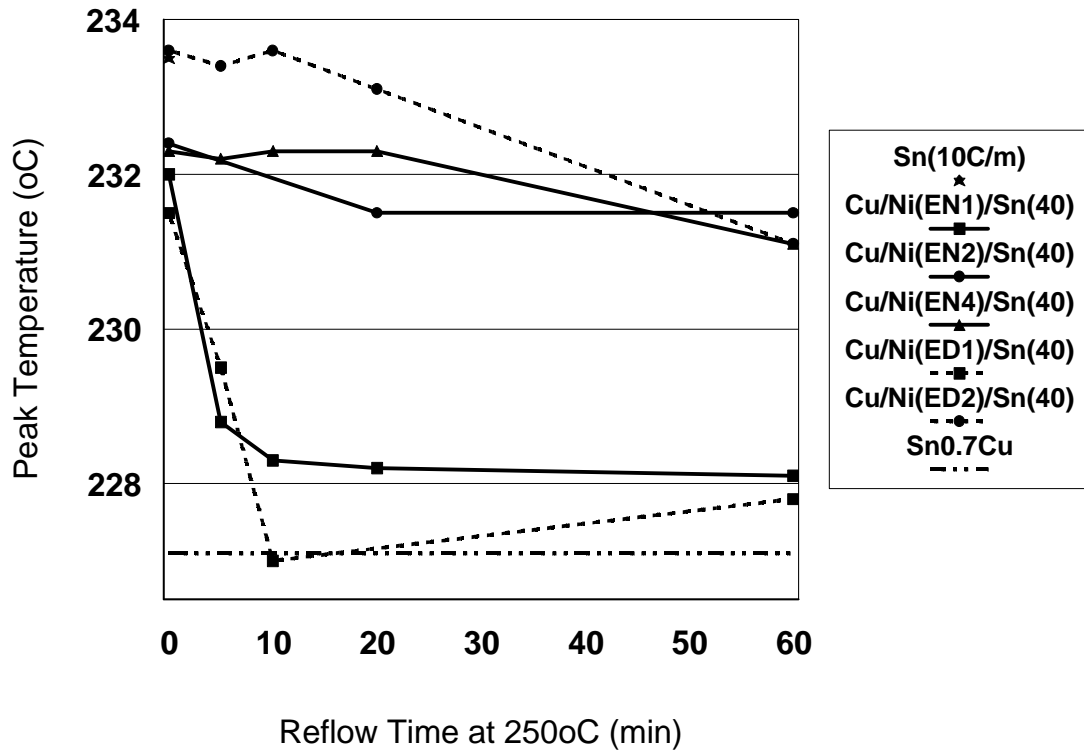


Figure 5 Energy Dispersive X-ray spectra from the cross-sectioned samples ; (a) 5  $\mu\text{m}$ , and (b) 40  $\mu\text{m}$  Sn.



**Figure 6** The variation of melting temperatures in Cu/Sn(40) balls as a function of reflow time.



**Figure 7** The Variation of melting temperatures in Cu/Sn balls with an electrolytic Ni and electroless Ni-P layers as a function of reflow time and Ni layer thickness.

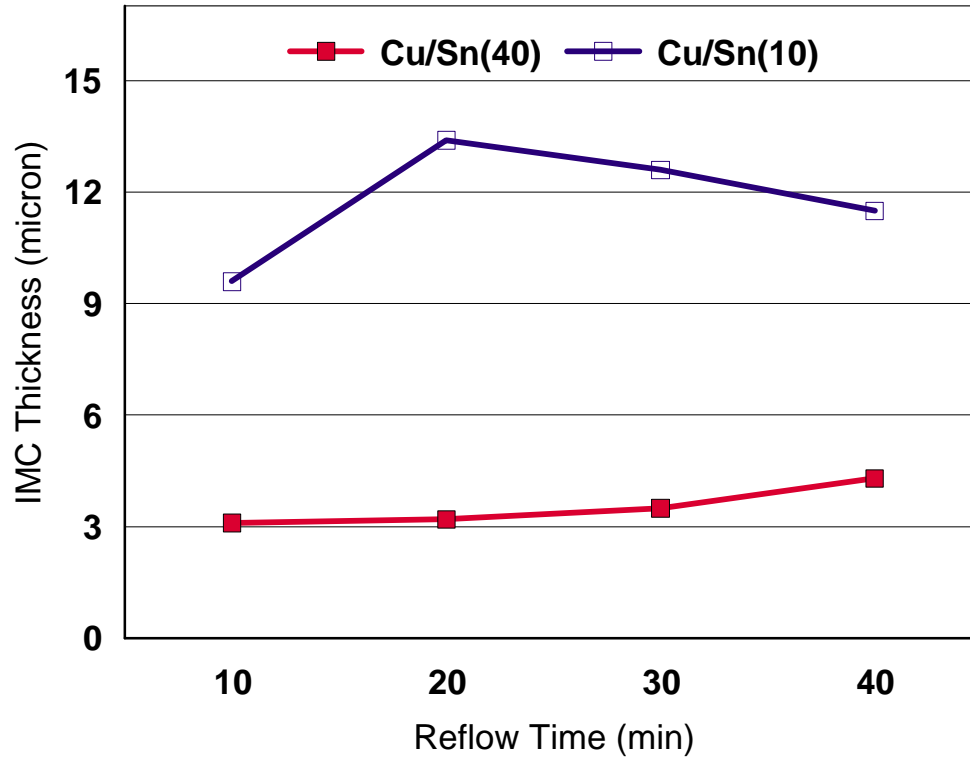


**Figure 8** The thickness of the  $\eta$ -Cu<sub>6</sub>Sn<sub>5</sub> phase formed at 250 °C as a function of reflow time in Cu/Sn(10) and Cu/Sn(40).

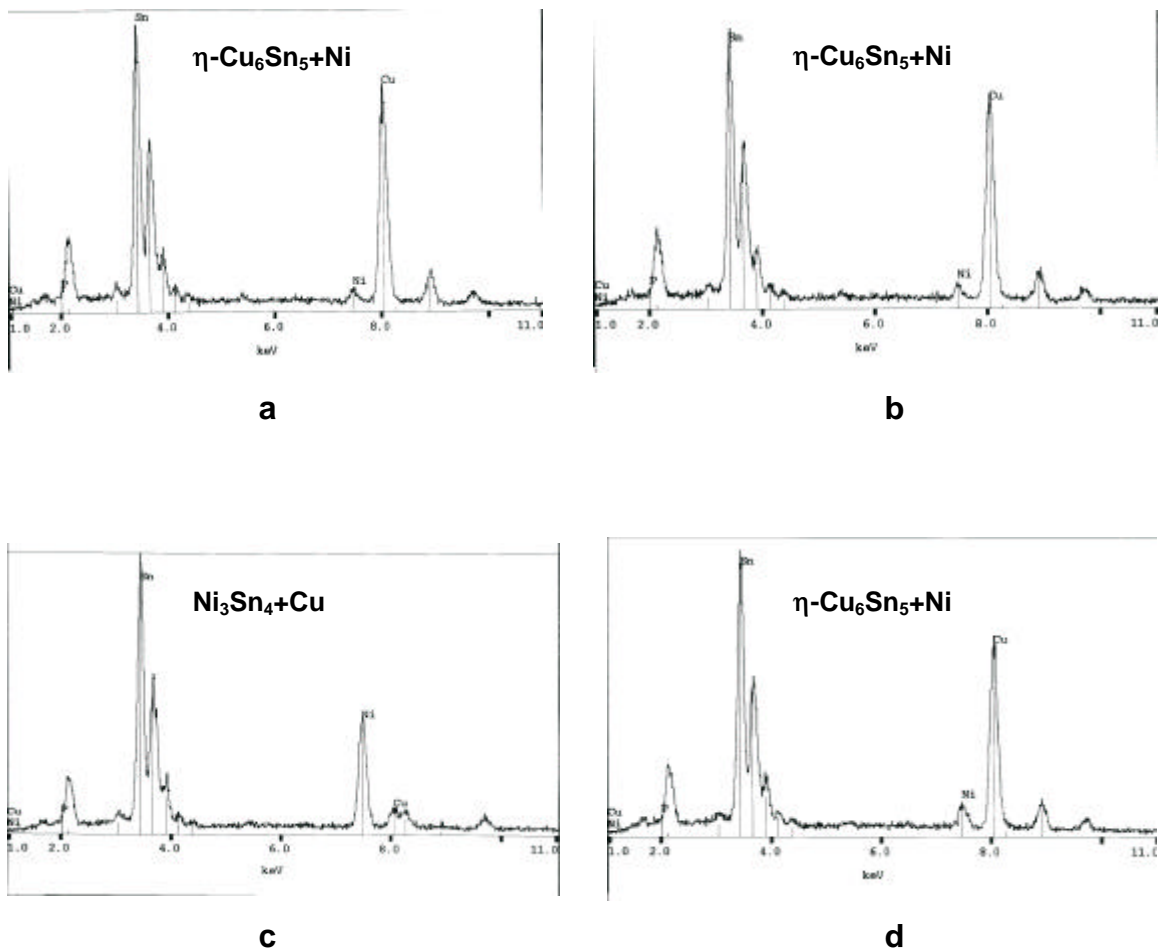


**Figure 9** EDS spectra of IMCs in Cu/Ni(ED1)/Sn after (a) 20 min and (b) 60 min, and in Cu/Ni(ED2)/Sn after (c) 20 min, and (d) 60 min.